

Post-Seismic Capacity of Damaged and Repaired Reinforced Concrete Plastic Hinges Extracted from a Real Building

A.Cuevas & S.Pampanin

Civil and Natural Resources Engineering Department, University of Canterbury, Christchurch, New Zealand.

Department of Structural and Geotechnical Engineering, La Sapienza University of Rome, Italy.



2017 NZSEE
Conference

ABSTRACT: This paper presents preliminary results of an experimental campaign on three beam-column joint subassemblies extracted from a 22-storey reinforced concrete frame building constructed in late 1980s at the Christchurch's Central Business District (CBD) area, damaged and demolished after the 2010-2011 Canterbury earthquakes sequence (CES). The building was designed following capacity design principles. Column sway (i.e., soft storey) mechanisms were avoided, and the beams were provided with plastic hinge relocation details at both beam-ends, aiming at developing plastic hinges away from the column faces. The specimens were tested under quasi-static cyclic displacement controlled lateral loading. One of the specimens, showing no visible residual cracks was cyclically tested in its as-is condition. The other two specimens which showed residual cracks varying between hairline and 1.0mm in width, were subjected to cyclic loading to simulate cracking patterns consistent with what can be considered moderate damage. The cracked specimens were then repaired with an epoxy injection technique and subsequently retested until reaching failure. The epoxy injection techniques demonstrated to be quite efficient in partly, although not fully, restoring the energy dissipation capacities of the damaged specimens at all beam rotation levels. The stiffness was partly restored within the elastic range and almost fully restored after the onset of nonlinear behaviour.

1 INTRODUCTION

Structures designed following modern (i.e. 1980s, post capacity design principles) codes are supposed to withstand major earthquakes by developing inelastic action and energy dissipation in concentrated regions referred to as plastic hinges. Therefore, and consistently with the current seismic performance-based design guidelines (SEAOC, 1995), structural damage is expected to occur. In particular and in very simple terms, modern structures should be capable of remaining fully operational (i.e. with negligible structural and non-structural damage) after frequent earthquakes, operational (i.e. with some non-structural damage without significant structural damage) after occasional ones, and allow for life safety (i.e. without collapsing) during a rare or design level earthquake.

The above philosophy implicitly means that modern structures should also be able to withstand several frequent and/or occasional earthquakes over their life span, and that they might suffer some level (minor-to-moderate) of damage and require some post-earthquake structural and non-structural repairs. Interestingly enough, one of the most controversial issues highlighted by the 2010-2011 Christchurch earthquakes sequence (CES) has been the lack of: a) comprehensive and robust guidelines to assess the residual capacity of damaged modern buildings, as well as b) in depth and evidence-based knowledge for selection and implementation of a reliable repairing technique capable of bringing (either totally or partially) the structure back to its pre-earthquake condition. Arguably, partly (although not exclusively) as a result of such lack of knowledge and guidelines, many modern buildings, in a number exceeding typical expectations from past experience at international levels, have ended up being demolished.

As part of an ongoing research project aiming at investigating the seismic residual capacity of reinforced concrete structures, this paper presents preliminary results of an experimental campaign on

three “modern designed” beam-column joints extracted from a 1980s multi-storey reinforced concrete frame building. The main objectives of the overall project were: a) the evaluation of the residual capacity of existing reinforced concrete buildings to sustain subsequent aftershocks and/or other design level earthquake during the remaining life of the building, and b) the identification and better understanding of the effectiveness of epoxy injection techniques, widely proposed and adopted in practice, for partly or fully restoring the seismic capacity of moderately damaged reinforced concrete members.

2 BUILDING DESCRIPTION AND OBSERVED DAMAGE

The PWC building (see Figure 1) was a 22-storey structure located on Armagh Street in the Christchurch’s Central Business (CBD) area. The lateral system comprised precast perimeter reinforced concrete (RC) frames with wet joints (typical of emulation of cast-in-place approach) in the beams at mid-span. The gravity system comprised precast double-tees with a reinforced concrete topping, supported on steel beams and concrete columns. The foundation system consisted of raft foundations. It was designed following capacity design principles and built in the 1980s. The perimeter frames had a hoop detail in the beam-ends intended to relocate the plastic hinge 500 mm away from the column face, so to avoid excessive demand and damage at the beam-column joint.

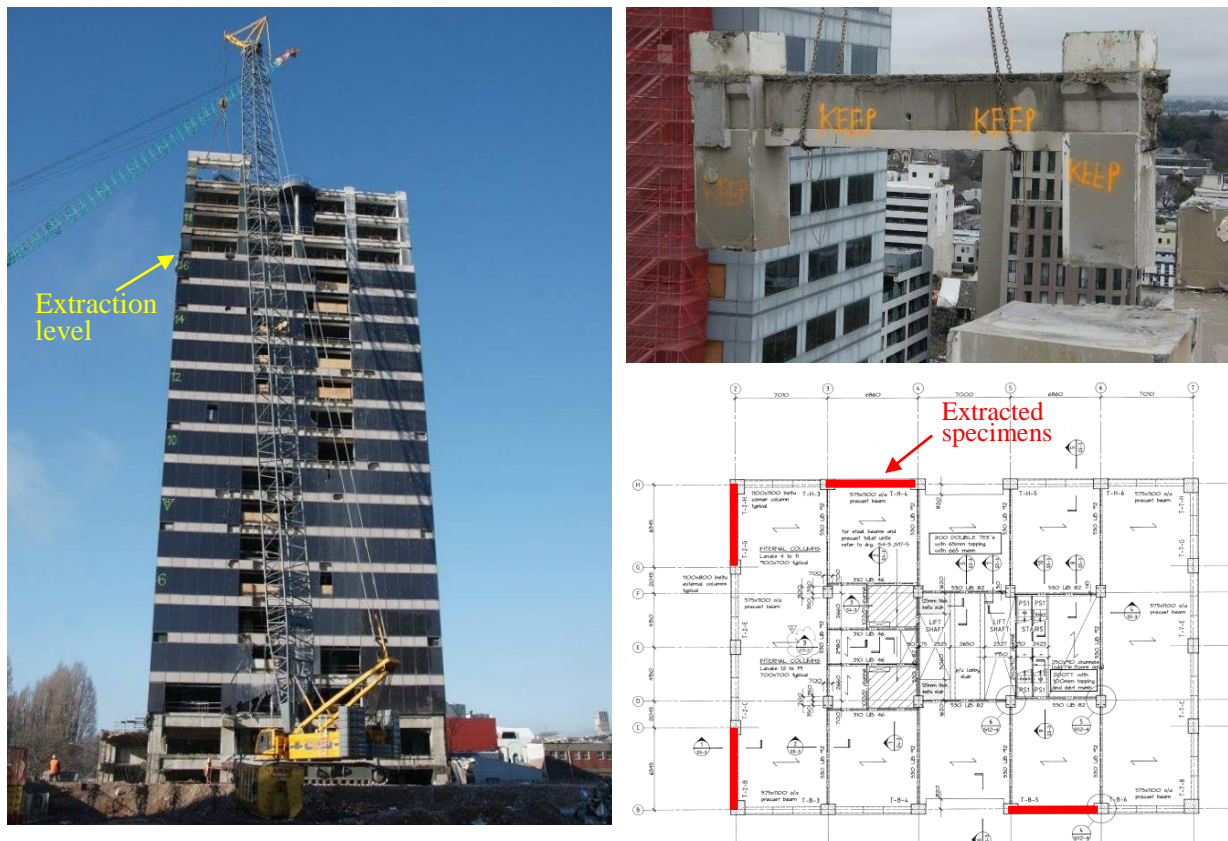


Figure 1. Elevation of the PWC building during the deconstruction process (left); extraction of one of the “H frames” (upper-right); typical floor plan view at the upper levels (lower-right), red lines indicate locations where the specimens were taken out of the 16th floor level.

During the CES, the building appeared to behave as expected, with the beams developing plastic hinges at both ends along the full height of the structure, with a general trend of diminishing level of damage along the elevation. The columns or joints did not show any signs of damage. The building experienced more damaged in the EW direction, consistent with the direction of the strongest components recorded in the surrounding area. Maximum observed residual cracks varied between 0.8 mm and 20 mm wide in the EW direction, and between 0.4 mm and 8 mm in the NS direction. Interestingly enough, most of the observed cracks were within, instead of outside, the plastic hinge

relocation detail (see Figure 2) which thus apparently did not work as intended per the original design. Residual drifts and tilting (due to liquefaction and lateral spreading) were also observed. More detailed information on the observed damage can be obtained in Giorgini et al. (2013) and Fleishman et al. (2014). The building was considered uneconomical to be repaired and consequently demolished in 2012. Four “H frames” were extracted from the 16th floor level during the demolition process for experimental purposes (see Figure 1).



Figure 2. Typical damage observed in the superstructure of the PWC building, level 9 interior unit H4 (left) and level 4 corner unit H2 (right) (Fleishman et al., 2014).

3 EXPERIMENTAL INVESTIGATION

3.1 Test Specimens

The “H frames” extracted during the deconstruction process were later cut in two “T-shape” specimens due to laboratory crane capacity limitations. Each of the “T-shape” specimens tested weighs between 10.5 ton and 13 ton. The beams are 2550 mm long (measured from the column face to the point of load application), 575 mm wide by 1100 mm high. The (main) longitudinal reinforcement consists of top and bottom 4 D-28 straight bars and 2 additional D28 hooked bars (within the plastic hinge relocation detail); the transverse reinforcement consists of 2 R-12 stirrups (one interior, one exterior) spaced at 150 mm crs. There is also secondary reinforcement detailed such that it provides vertical support to the flooring system (see Figure 3). The columns are 2700 mm long, either 1100 mm square (at the building’s corners) or 1100 mm by 800 mm (at the building’s interior columns). The nominal steel yield strength and concrete compressive strengths, as specified in the drawings, are 300 MPa and 30 MPa, respectively.

3.2 Experimental Program

Three beam column joints out of the eight extracted (i.e. four “H” frames) were initially tested at this stage. The first specimen corresponds to one of the frames oriented in the N-S direction, with no visible residual cracks and consequently considered as slightly damaged. The specimen was subjected to a standard quasi-static reverse cyclic testing loading protocol (described in the following section) up to a maximum “total” (see Section 3.3) rotation of 2.5% (Test 1).

The second specimen corresponds to one of the frames oriented in the EW direction, in which the building experienced more damage. Residual cracks varying between hairline and 0.8mm in width were observed prior to the test. The specimen was subjected to the same standard loading protocol up to a maximum “total” rotation of 1% (Test 2.1), enough to re-activate all the existing cracks and develop residual (static) cracks between 0.1 mm and 2.0 mm in width. The specimen was subsequently repaired by epoxy pressure injection, one of the most typical repairing techniques (to the authors’ knowledge) that has been proposed and/or applied in Christchurch following the CES. The repaired specimen was retested again following the same loading protocol until reaching complete failure (Test 2.2).

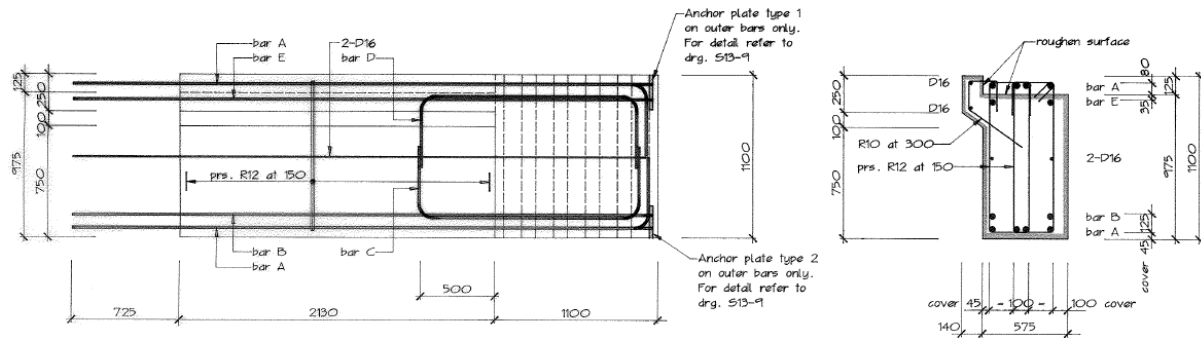


Figure 3. Typical section and elevation view of beams tested (Holmes Consulting Group).

The third and last specimen corresponds to the second half of the “H frame” where the second specimen was extracted from. Residual cracks varying between hairline and 1.0 mm in width were observed prior to the test. The specimen was subjected to the standard loading protocol up to a maximum “total” rotation of 1.5% (Test 3.1), enough to re-activate all the existing cracks and develop new ones with residual (static) cracks between 0.1 mm and 6 mm in width. The specimen was subsequently repaired by epoxy pressure injection, and retested again following the same loading protocol until reaching complete failure (Test 3.2).

Table 1. Summary of the experimental program.

	Observed (pre-test) Damage		Max. Beam Rotation
Test 1 (N-S)	No visible residual cracks		2.5 %
Test 2 (E-W)	Test 2.1	Hairline – 0.8 mm	1.0 %
	Test 2.2	0.1 mm – 2.0 mm	4.5 %
Test 3 (E-W)	Test 3.1	Hairline – 1.0 mm	1.5 %
	Test 3.2	0.1 mm – 6.0 mm	4.5 %

3.3 Testing Procedure and Instrumentation

As shown in Figure 4, the reaction frame used for the tests consisted of steel braced frames anchored to the RC strong floor. The beam-column joint was placed horizontally on top of steel beams and clamped to the braced frames with steel channels and post-tensioned Macalloy bars. The beam-end was vertically supported on Teflon pads. A steel frame with a roller prevented the beam-end to uplift due to any accidental eccentricity that might occur at the actuator-to-beam connection. No axial and gravity loads were applied at the column (in addition to the resultant force from the post-tensioned bars) and beam, respectively.

The actuator was located approximately at the theoretical inflection point at mid-span of the beams oriented in the NS direction of the building. A quasi-static displacement-controlled cycling loading protocol was applied at the beam-end (increasing “total” beam rotations of $\pm 0.1\%$, $\pm 0.2\%$, $\pm 0.5\%$, $\pm 0.75\%$, $\pm 1.0\%$, $\pm 1.5\%$, $\pm 2.0\%$, $\pm 2.5\%$, $\pm 3.5\%$, and $\pm 4.5\%$, see Figure 10) as per the acceptance criteria of the American Concrete Institute (ACI, 2001).

The instrumentation consisted of 33 linear potentiometers for measuring displacements at different points along the beam and beam-column joint (required for further estimation of rotations and shear deformations), 1 load cell for measuring the applied load in the actuator, and 2 rotational potentiometers at the beam-end for measuring beam elongation and applied displacements. During the deconstruction process, the beams adjacent to the extracted “H frames” were cut-off at the column face, approx. Therefore, in some of the specimens the flexural beam capacity relies upon straight D28 bars developed over a length of 1100 mm (i.e. without a standard hook), just above the minimum required. Two spring potentiometers were located at the bars at the cut-off section for measuring bar slips during the test, if any.

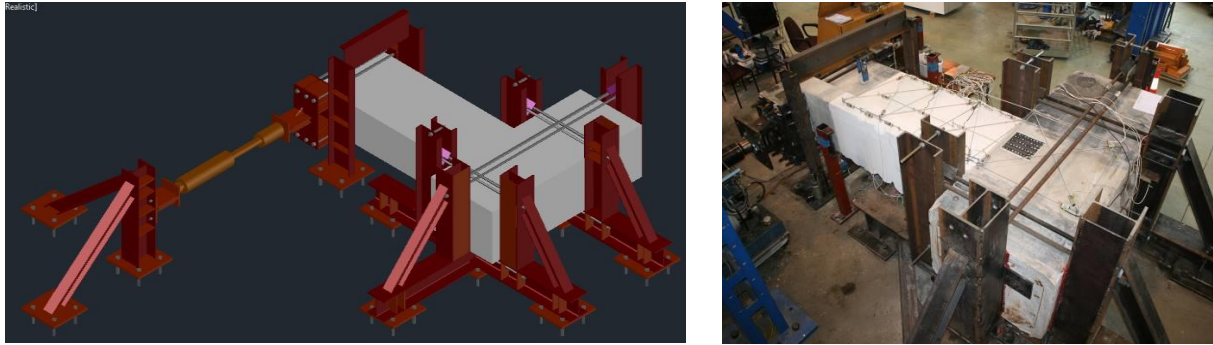


Figure 4. 3D CAD view of the reaction frame (left); specimen 1 during the tests (right).

Three additional rotary potentiometers were strategically installed to capture rigid body translations and rotations of the specimen (due to axial elongation of the post-tensioned bars, slip at the reaction frame-to-strong floor connections, the specimen setup, and any other deformation in the reaction frame that might occur during the test). This translation and rotation is further translated into an equivalent lateral displacement at the beam-end and extracted from the “total” applied displacement.

3.4 Epoxy Repairs

The commercial epoxy Sikadur 52 was used in the specimens’ repairs. As per the manufacturer’s specification, it is a solvent free, non-shrinkage, two component low-viscosity liquid based on high strength epoxy resins, suitable for injecting cracks from 0.2 mm-to-5.0 mm wide. The pot life (at 20 °C) is 20 min. It develops compressive strengths of 45 MPa after 7 days (at 20 °C) and tensile strengths of 25 MPa, approximately. The bond strength in sandblasted concrete is as high as 3.5 MPa, approximately.

The repair works were conducted by BBR CONTECH, concrete specialists with broad experience on epoxy injection repairs in Christchurch following the CES, with the technical support from the product manufacturer. As shown in Figure 5, the damaged specimens were repaired in the same horizontal position as they were tested. The repair process started with grinding the surface along the crack lines to seal them with a well bonded epoxy mortar. It was necessary to seal both sides of the crack to prevent leakage. Injection ports were simultaneously installed at 100-200 mm crs. (sometimes closer depending on the cracking pattern). The epoxy material was mixed and the resin was injected under pressure via the injection ports through an air-operated pressure pump. The injection port was sequentially interchanged to allow the resin to travel and fill the interior cracks. The ports were sealed as the resin started leaking through them. Once the injection process was finished, the surface was cleaned off by removing the hardened epoxy mortar, leaving the surface flush. A total 4.8 L and 10.9 L of resin injected at 34.5 MPa (5 psi) were required to repair the specimens 2 and 3, respectively.

4 EXPERIMENTAL RESULTS

4.1 Global Response

4.1.1 Test 1

Cracks of 0.1mm in width opened up at 0.2% “total” beam rotation. These cracks might be pre-existing ones (earthquake induced) that closed due to the low level of inelastic action. At 1.5% total rotation most of the deformation was concentrated at a single diagonal crack 4-12 mm wide (see Figure 6), and shear distortions became more evident. The reason of these diagonal cracks could be excessive principal tensile stresses as a result of the diagonal compression strut induced by the hooked bars within the plastic hinge relocation detail. It was not possible to test the specimen up to failure due to the excessive and unexpected shear deformation (and sliding shear mechanism) of the specimen. The reaction frame was later modified in order to accommodate such displacement.

Worth noting that some of the specimens were also part of the structure’s gravity system, and the

inclusion of the gravity load effect during the test would have triggered the specimen's shear failure at an earlier stage.



Figure 5. Epoxy repairs in specimen 3. Sealing process with epoxy mortar and installation of injection ports (upper-left); resin injection with an air-operated pump (upper-right); epoxy resin leaking from and sealing of the injection ports (lower-left); finish once the epoxy mortar has been removed (lower-right).

4.1.2 Test 2.1

Cracks 0.1 mm wide were also observed at 0.2% “total” beam rotation. Maximum cracks of 3 mm in width were observed at 1% “total” beam rotation (see Figure 7). By comparing the cracking pattern before and after the test, it is believed that most of the (earthquake) pre-existing cracks were activated at this beam rotation level. Residual (static) cracks between 0.1 mm and 2.0 mm in width were observed at the end of the test.

4.1.3 Test 2.2

Cracks of 0.1-0.2 mm in width started developing at 0.1% “total” beam rotation. A new crack extended from the column face towards the interior of the joint, and did not follow the injected crack path. At 0.75% “total” beam rotation, 0.1 mm-hairline cracks started developing outside the plastic hinge relocation detail. At beam rotations of 1.5%, residual (static) cracks started becoming comparable to the maximum observed (70-90% of the maximum crack width). Maximum cracks of 9-18 mm in width were observed at 2.5% “total” beam rotation. As shown in Figure 7, most of the repaired cracks re-opened up during the Test 2.2.

4.1.4 Test 3.1

Existing cracks 0.1-0.15 mm wide opened up at 0.1% “total” beam rotation. The cracks continued increasing in quantity and in width, reaching 7 mm at 1.5% “total” beam rotation. As in the Test 2.2, residual cracks started becoming comparable to the maximum observed at this beam rotation level. Some sliding with diagonal cracking was observed at the wet joint close to the mid-span. Residual (static) cracks between 0.1 mm and 6 mm in width were observed at the end of the test.

4.1.5 Test 3.2

Cracks 0.1 mm wide were observed at 0.1% “total” beam rotation. Sliding and diagonal cracking was observed at the cold joint, even at such low rotation level. New flexural cracks were observed outside the plastic hinge relocation detail. As in the Test 3.1, residual (diagonal) cracks started becoming comparable to the maximum observed at 1.5% “total” beam rotation level. Maximum cracks of 10mm in width were observed at 2.5% beam rotation. As shown in Figure 8, most of the repaired cracks opened up during the Test 3.2.

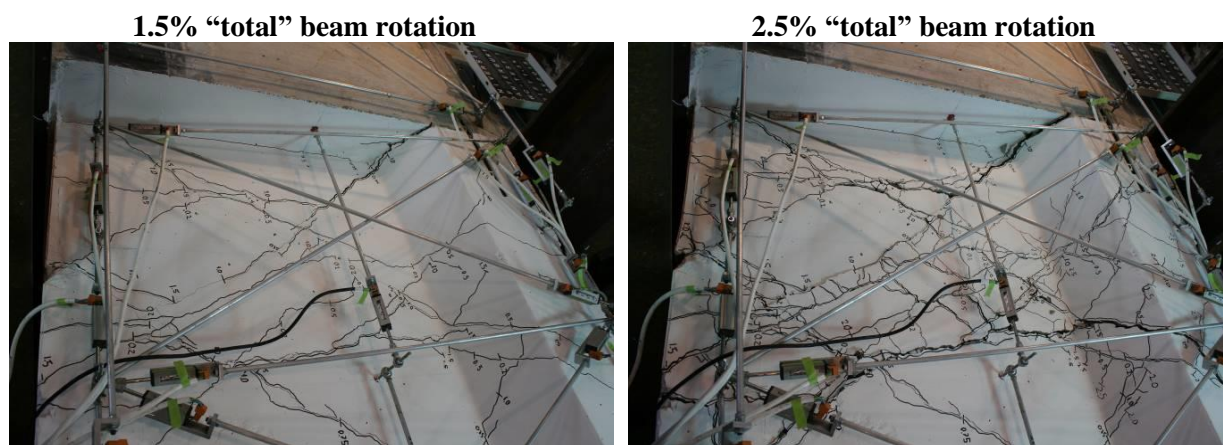


Figure 6. Residual racking pattern observed during Test 1, at 1.5% and 2.5% “total” beam rotation.

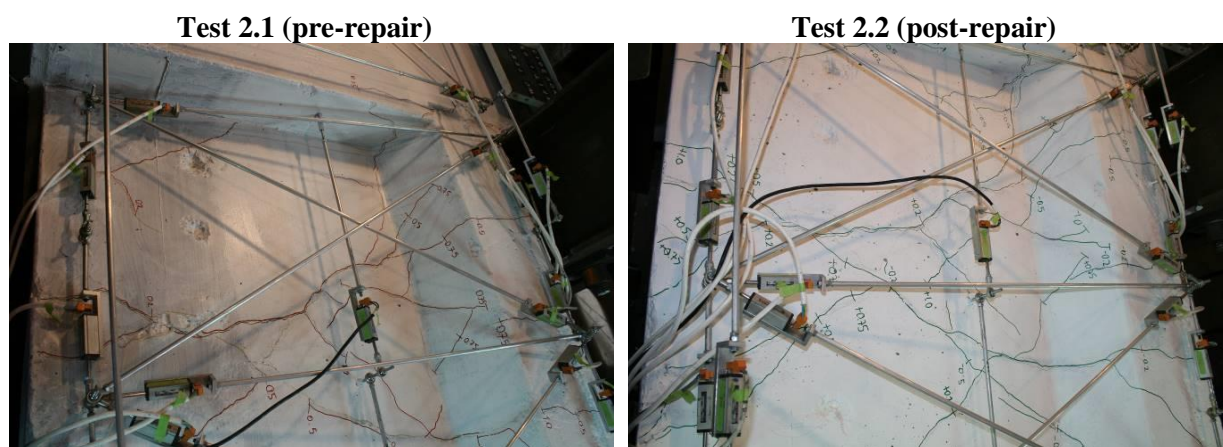


Figure 7. Residual cracking pattern observed during Test 2 at 1.0% “total” beam rotation.

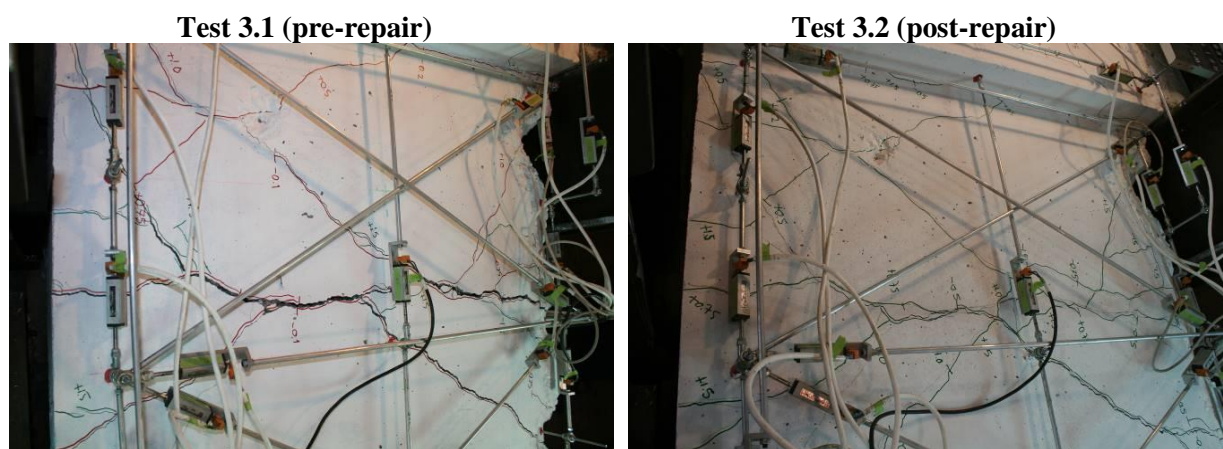


Figure 8. Residual cracking pattern observed during Test 3 at 1.5% “total” beam rotation.

Figure 9 shows cracking patterns in Tests 1, 2.2 and 3.2, at different levels of “total” beam rotation. It is evident that the damage in Test 2.1 is more severe at lower (below 1.5%) rotation levels. Test 1

experienced the most severe damage at 2.5%, while Test 3.2 experienced the less damage at all rotation levels, with some of the damage in the form of flexural cracks outside the plastic hinge relocation detail.

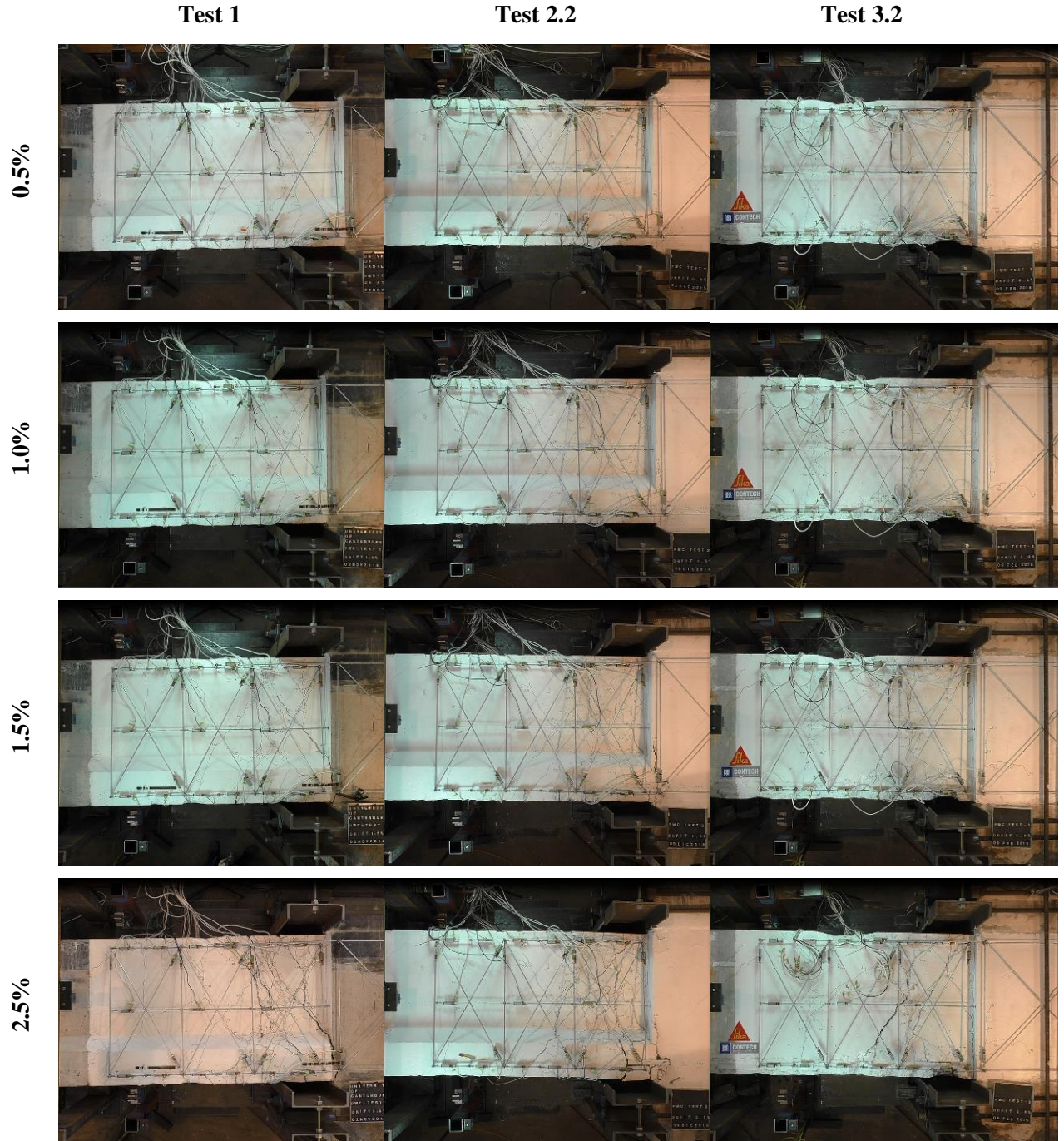


Figure 9. Observed damaged at different beam rotations (in “total” displacement units).

In Figure 10, solid grey lines represent force-displacement curves measured in “total” displacement units, whereas solid black lines are in “effective” displacement units (i.e., the “total” applied displacement minus the equivalent lateral displacement at the beam end due to rigid body translation and rotation). The onset of nonlinearity occurs at about 0.5% “effective” beam rotation. Rotation ductility demands of around 1.20 and 2.10 were achieved at the end of Tests 2.1 and 3.1, respectively.

All the tests show a relatively stable hysteretic behaviour at early stages, with however a sudden drop in strength during the last 3 cycles in both repaired configurations (Tests 2.2 and 3.2). Higher pinching behaviour, due to cracks opening and closing and more likely due to bond-slip degradation, was observed in the repaired configurations, in particular for Test 2.2.

When considering Test 3.2, the relocation of cracks outside the plastic hinge relocation detail led to higher shear forces for the same displacement demand and a more stable hysteresis loop with less pinching. Overall, the effective displacement (capacity) achieved in the test was lower than in other tests.

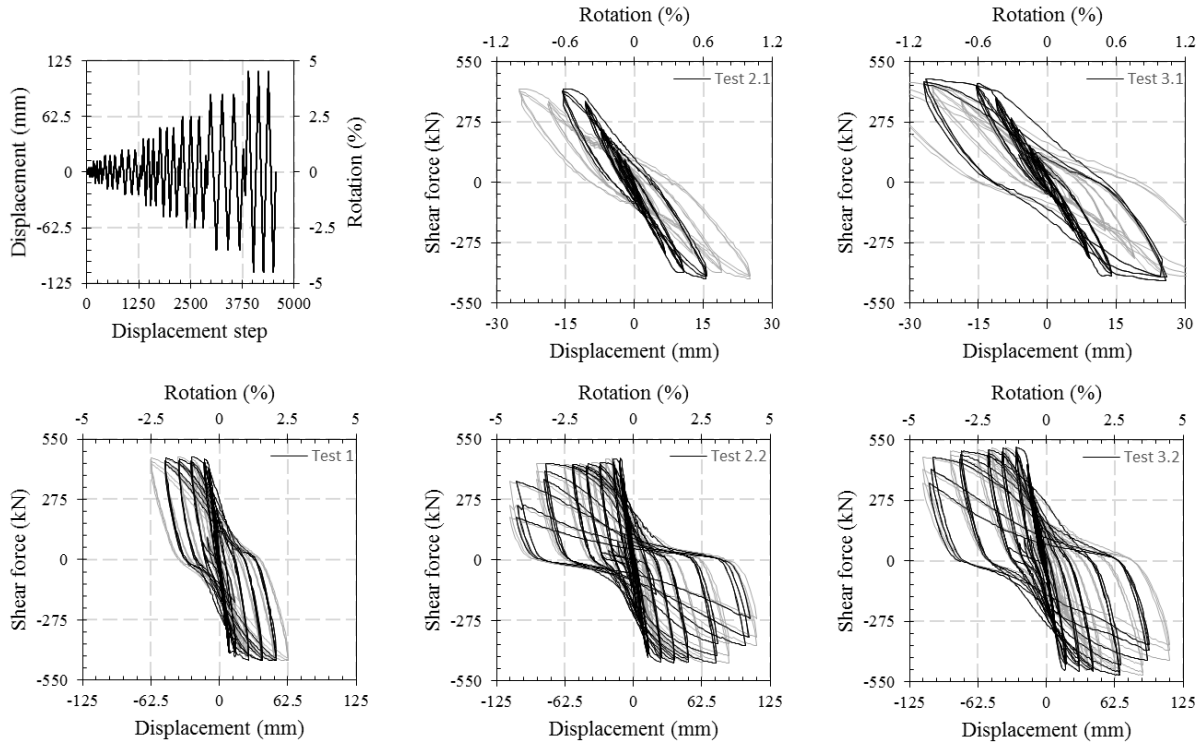


Figure 10. Applied loading protocol (upper-left), and force-displacement curves.

Figure 11 shows the axial beam elongation for all the tests. It can be noted that the beam elongation is permanent and cumulative. Maximum elongations in Tests 2.1 and 2.2 were 2 mm and 7.2 mm, respectively, equivalent to 0.08% and 0.29% increase in beam length. These beam elongations were consistent with the maximum cracks widths observed at the end of the tests. Maximum elongations in Tests 1, 2.2 and 3.2 were 21mm, 26mm, and 30mm, equivalent to 0.85%, 1.05%, and 1.20% increase in beam length, respectively. It is worth noting that the testing apparatus allowed for free beam elongation without any restraint action from the floor diaphragm as in fact would occur in the real building. Therefore, while the results are important to develop a better understanding of the behaviour of a “free” subassemblies, the beam elongation results are not fully representative of what we would have observed following the earthquakes.

4.2 Energy Dissipation and Stiffness Degradation Characteristics

Figure 12 (top) shows cumulative energy dissipation computed as the sum of the area enclosed within the force-displacement curves, computed in “effective” displacement units. As shown in the figures, more energy is dissipated in Test 3.2 than in Test 2.2 (and arguably more than in Test 1 if we can infer that following the trend in the graph). This can be attributable to the less pinching as a result of more damage relocation (flexural type, outside the plastic hinge relocation detail). In general, reasonably good energy dissipation at both low (SLS) and high (ULS) rotation levels was achieved in the repaired specimens when compared with the slightly damaged specimen (Test 1).

Figure 12 (bottom) shows “peak-to-peak” secant stiffness for the first loading cycles, computed in “effective” displacement units as the slope of the line joining the maximum and minimum peaks in the force-displacement curves at each of the beam rotation levels.

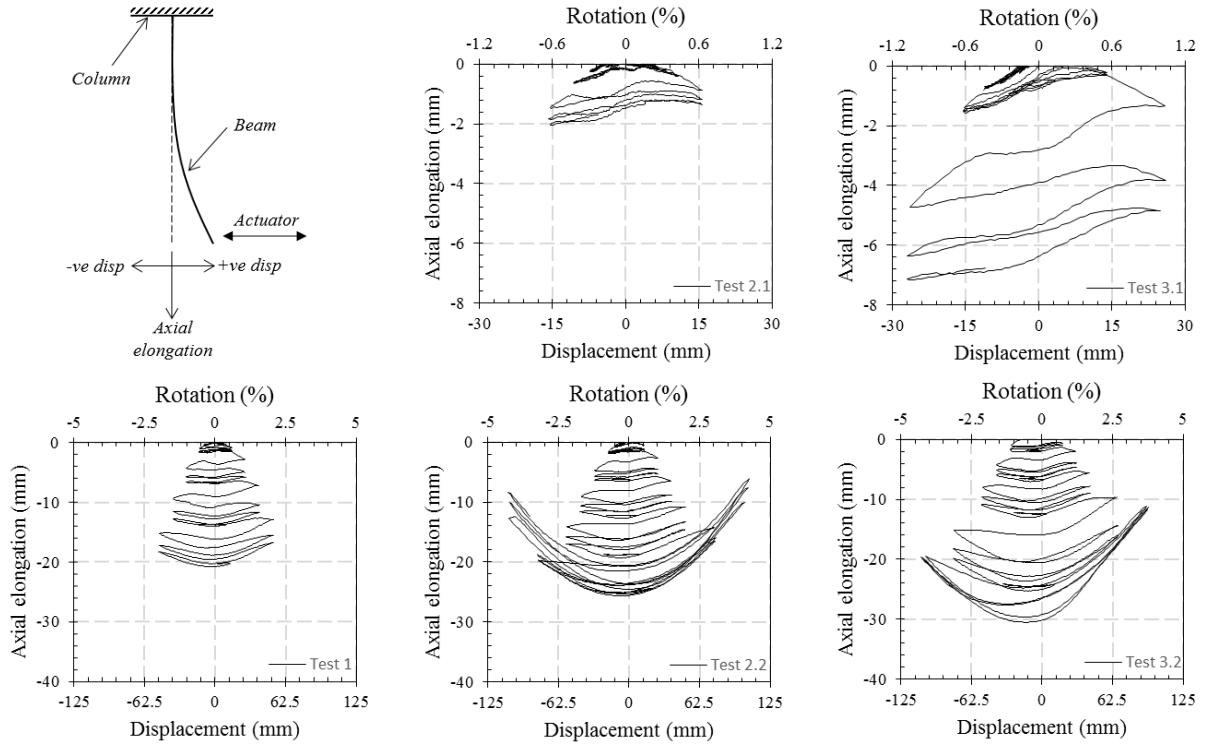


Figure 11. Displacement sign convention (upper-left), and beam elongation curves.

As shown in the figures, there is a reduction of stiffness in the repaired specimens (both Test 2.2 and 3.2) at low rotation levels (below to the onset of nonlinearity, approximately) when compared with the slightly damaged specimen (Test 1). There is a better stiffness recovering (at low rotation levels) in Test 2.2 than in 3.2, possibly because of its lower damage condition prior to the repairs. The secant stiffness of Test 2.2 is also closer to the one obtained in Test 1, and the same in Test 2.1. In general, the secant stiffness does not seem to be significantly affected at high (ULS) rotation levels when compared with Test 1.

4.3 Crack Widths Investigation

Figure 13 shows maximum and (static) residual crack widths measured during the tests. The top figures correspond to the most critical crack(s) observed within the plastic hinge relocation detail (i.e., shear-flexural cracks); the bottom ones correspond to flexural cracks observed outside the plastic hinge relocation detail during the Test 3.2. The maximum crack widths are measured at peak force, whilst the residual crack widths at zero force. Worth reminding that these residual cracks are “static” ones. The dynamics effects during the earthquake, as well as any axial load contribution, i.e. slab engagement effect resisting to the beam elongation, would further reduce them, thus increasing the maximum/residual ratio (Christopoulos et al., 2003; Pampanin et al., 2003).

Crack width ratios computed as the residual crack width upon the maximum residual crack width are also shown in the figure. It is evident how the crack width ratios are rotation (i.e. drift) dependant, showing a change of slope from negative to positive at rotations near or at the onset of nonlinearity. The negative slopes below the onset of nonlinearity are due to the fact that at low rotation levels the residual cracks are very small and almost constant (hairline-to-0.1 mm in width), regardless of the increase of the maximum crack widths as the rotation level increases. This is in line with recent post-earthquake observations (Pampanin et al., 2012; SESOC, 2011) where hairline-minor residual crack width could in fact hide non-negligible, if not significant, damage, including tensile fracture of the bars, especially in lightly reinforced shear walls.

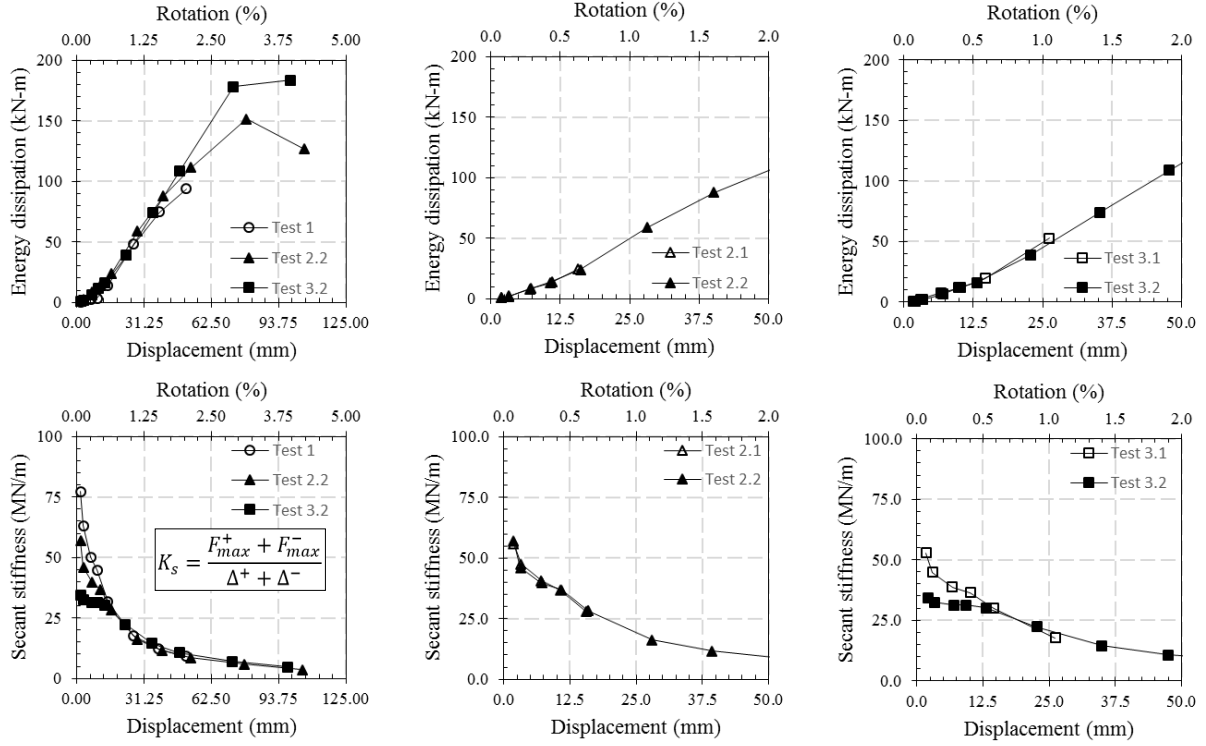


Figure 12. Energy dissipation (top) and secant stiffness degradation at 1st cycles (bottom) characteristics.

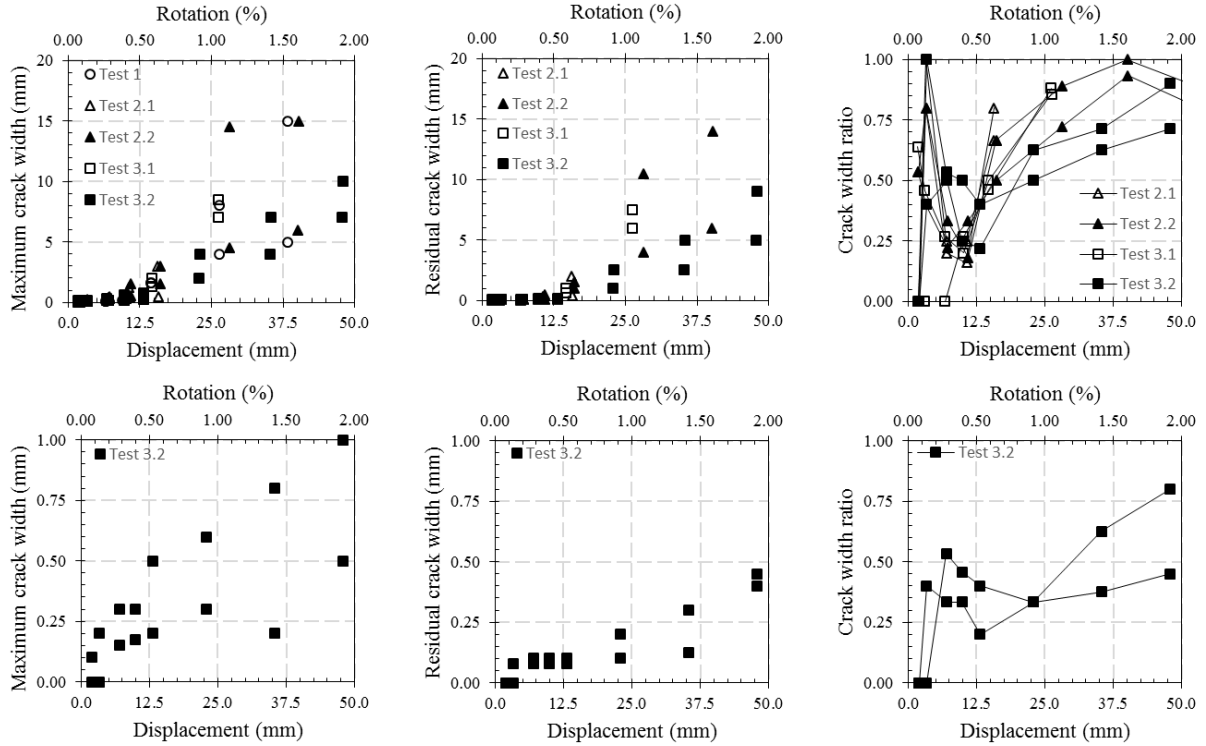


Figure 13. Maximum and residual cracks, and crack width ratios within (top) and outside (bottom) the plastic hinge relocation detail.

5 SUMMARY AND CONCLUSIONS

This paper presents preliminary results of an experimental campaign on three modern designed beam-column joints extracted from a 1980s 22-storey reinforced concrete frame building in the Christchurch's Central Business District (CBD), damaged after the 2010-2011 Christchurch

earthquakes sequence (CES). Two of the specimens were tested under quasi-static cyclic loading to a level of cracking pattern consistent with what can be considered a moderate level of damage, repaired with an epoxy injection technique, and subsequently retested until reaching failure. The main observations can be summarised as follows:

- All the specimens failed in a flexure-shear mechanism. Severe diagonal cracking was developed within the plastic hinge relocation detail due to excessive principal tensile stresses as a result of the diagonal compression strut induced by the hooked bars details. In the repaired specimens 2.2, and more clearly in 3.2, the epoxy injection allowed for some damage relocation outside the plastic hinge relocation detail.
- A reasonable level of energy dissipation at both low (SLS) and high (ULS) rotation levels was achieved in the repaired specimens. The computed values are comparable to the ones from the unrepaired specimens. A secant stiffness reduction was observed in the repaired specimens at low rotation levels (below to the onset of nonlinearity, approximately). However, this stiffness reduction does not seem to be equally affected at high (ULS) rotation levels.
- The crack width ratios (for both, shear-flexural or flexural only) are beam rotation (i.e., drift) dependant. There is a change from negative to positive slopes at rotations near or at the onset of nonlinearity. In fact, negligible-to-minor residual cracks can derive from non-negligible level of maximum crack width.

6 ACKNOWLEDGEMENTS

This research investigation was sponsored by the Natural Hazards Research Platform (NHRP). The collaboration of Daniel Smith Industries, Arrow International and Nikau Group for extracting and preserving the specimens, as well as BBR CONTECH for all the epoxy repair works required during the tests is acknowledged.

7 REFERENCES

- Structural Engineers Association of California, SEAOC, Vision 2000 Committee. 1995. *Performance based seismic engineering of buildings*, Sacramento, California.
- Giorgini, S., Pampanin, S., Carr, A.J. & Cubrinovsky, M. 2013. *Seismic behaviour of a 22 storey building during the Canterbury earthquakes*. Proceedings of the 2013 NZSEE Conference, Wellington, New Zealand.
- Fleishman, R.B., Restrepo, J.I., Pampanin, S., Maffei, J.R., Seeber, K. & Zahn F.A. 2014. *Damage evaluations of precast concrete structures in the 2010-2011 Canterbury earthquake sequence*. Earthquake Spectra, 30 (1), 277-306.
- Holmes Consulting Group: Price Waterhouse Centre. Structural drawings, issued for construction.
- ACI. 2001. *Acceptance Criteria for Moment Frames Based on Structural Testing (T1.1-01) and Commentary (T1.1R-01)*. A. I. T. G. 1, ed., Farmington Hills, Michigan.
- Christopoulos, C., Pampanin, S. & Priestley, M.J.N. 2003. *Performance-based seismic response of frame structures including residual deformations. Part 1: Single-degree of freedom systems*. Journal of Earthquake Engineering, 7 (1), 97-118.
- Pampanin, S., Christopoulos, C. & Priestley, M.J.N. 2003. *Performance-based seismic response of frame structures including residual deformations. Part 2: Multi-degree of freedom systems*. Journal of Earthquake Engineering, 7 (1), 119-147.
- Pampanin, S., Kam, W.Y., Akguzel, U., Tasligedik, A.S. & Quintana-Gallo, P. 2012. *Seismic performance of reinforced concrete buildings in the Christchurch CBD in 22 February 2011 earthquake. Part I and II*. Natural Hazards Research Platform, Recovery Project. University of Canterbury, Christchurch, New Zealand.
- SESOC. 2011. *Preliminary observations from Christchurch earthquakes*. Structural Engineering Society New Zealand, Auckland, New Zealand.